Application of Sandwich Plate System (SPS) on 155 m Barge: Framing System Configuration, Weight saving, and Dynamic Characteristic Assessment

Primjena sendvič panel sustava na 155 m barži (teglenici): konfiguracija konstrukcijskog sustava, smanjenje težine i procjena dinamičkih karakteristika

Tuswan Tuswan
Universitas Diponegoro
Department of Naval Architecture
Semarang, Indonesia
E-mail: tuswan@lecturer.undip.ac.id

Achmad Rezaldy
Universitas Diponegoro
Department of Naval Architecture
Semarang, Indonesia
E-mail: achmadrezaldy@students.undip.ac.id

Ocid Mursid*
Universitas Diponegoro
Department of Naval Architecture
Semarang, Indonesia
E-mail: ocidmursid@lecturer.undip.ac.id

Hartono Yudo
Universitas Diponegoro
Department of Naval Architecture
Semarang, Indonesia
E-mail: hartono.yudo@yahoo.com

Aditya Rio Prabowo
Universitas Sebelas Maret
Department of Mechanical Engineering
Surakarta, Indonesia
E-mail: aditya@ft.uns.ac.id

DOI 10.17818/NM/2023/1.6
UDK 629.5.015: 626.51
Professional paper / *Stručni rad*
Paper received / *Rukopis primljen:* 19. 12. 2022.
Paper accepted / *Rukopis prihvaćen:* 28. 2. 2023.

Abstract

The SPS application in ship structure is an innovative breakthrough that provides an excellent strength-to-weight ratio. SPS application for new construction is crucial to ensure the proposed design has better static and dynamic behavior than conventional design. The study aims to evaluate the weight savings and dynamic characteristics of different proposed framing systems of 155 m barge due to the application of various SPS types in the deck, ship hull, and bottom structures. A total of three proposed construction systems: longitudinal, transverse, and mixed framing systems, are investigated under different plate configurations, material types, and scantling sizes. In addition, the free vibration analysis is used to evaluate the influence of damage occurrence on the structural characteristics. Several damage parameters, including damage size, location, shape, and depth, are investigated using ABAQUS software. The promising result of weight saving indicates SPS application results in about 9-13%. Moreover, the debonding assessment reveals that eigenvalue decreases with increasing debonding size, where the damaging effect in higher modes is more substantial. The stiffness loss due to debonding causes a high local deformation in the debonded area. Moreover, interfacial debonding reduces eigenvalues significantly, particularly in localized debonding shapes. It can be found that several damage parameters, including damage size, location, depth, and shape, influence the eigenvalue shifts.

KEY WORDS
ship framing
barge
finite element
free vibration

Sažetak

Primjena sendvič panel sustava (SPS) u strukturi broda inovativno je rješenje koje omogućuje izvrstan omjer snage i težine. Primjena SPS-a na novoj konstrukciji ključna je kako bi se osiguralo da predložen dizajn ima bolju statiku i dinamiku od konvencionalnog dizajna. Cilj je ovoga istraživanja procijeniti uštede na težini i dinamičkim karakteristikama više predloženih konstrukcijskih sustava teglenice od 155 m primjenom različitih SPS tipova na palubi, trupu i dnu strukture. Ukupno su istražena tri predložena konstrukcijska sustava: longitudinalni, poprečni i miješani sustav konstrukcije, s različitim konfiguracijama oplate, tipovima materijala i veličinama propisanih mjera. Osim toga, koristi se analiza slobodne vibracije za procjenu utjecaja štetnih pojava na strukturne karakteristike. Nekoliko parametara oštećenja, uključujući veličinu oštećenja, mjesto, oblik i dubinu, ispitano je uporabom ABAQUS softvera. Obećavajući rezultat uštede na težini pokazuje da primjena SPS-a donosi uštedu od oko 9 – 13%. Osim toga, procjena otpuštanja otkriva da svojstvena vrijednost (eigenvalue) pada kako se površina otpuštanja povećava, dok je štetni učinak na višim modalitetima značajniji. Gubitak krutosti uslijed otpuštanja uzrokuje veliku lokalnu deformaciju u dijelu gdje se javlja otpuštanje. Povrh toga, procjenja otpuštanja uzrokuje velike deformacije na mjestima otpuštanja. Može se vidjeti da nekoliko parametara oštećenja, uključujući veličinu, lokaciju, dubinu i oblik, utječe na promjenu svojstvene vrijednosti (eigenvalue).

KLJUČNE RIJEČI
konstrukcija broda
teglenica
konačni element
slobodne vibracije

* Corresponding author

1. INTRODUCTION / *Uvod*

Shipping has built sophisticated logistics systems that deliver just-in-time parts and goods to manufacturers and consumers to support global economies. Ship is one of the essential transportation modes in commercial activity, providing passengers or commodities. The economic component of running a merchant ship is critical since a shipowner needs a vessel that maximizes his original investment while also covering his running costs. It indicates that the final design considers the economic conditions at the construction time and those likely to emerge during the ship's lifetime [1].

Utilizing lightweight materials for ship structures is one way to improve competition with other modes of transportation. Increased load-carrying capacity is a structural design and lightweight optimization goal in the shipbuilding industry. In order to enhance ship payload for specific ship sizes, achieve higher speed, and minimize fuel consumption and environmental emissions for a given payload and distance covered, many scholars are interested in adopting lightweight materials as ship structures. Lightweight structures can be produced by modifying the dimensions of already-built structures or incorporating lightweight materials into possible structural components. To anticipate unforeseen technical, practical, and financial difficulties during manufacturing and to ensure that applied materials are correctly used by a shipowner, classification societies, and management, weight savings should be consequential when applying lightweight material [2].

The development of lightweight materials for ship structural application has involved using various materials, from ancient materials like wood and cast iron to contemporary materials like steel, aluminum, and carbon fibre. Lightweight materials in ships are currently and potentially used primarily in high-speed passenger and car ferries, patrol and rescue craft, smaller naval ships, luxury craft, and sailing yachts. However, they are also utilized in the superstructures of larger navy ships and cruise ships (e.g., frigates). Additionally, they are widely used in non structural elements, such as decks, mobile vehicle ramps, and masts and casings.

In applying lightweight material, ship components must be strong and as light as possible. It is typically challenging to accomplish because strong materials are often heavy, and lightweight materials frequently have low strength values. One of the solutions to the aforementioned concerns is the usage of sandwich plates, which combine the arrangement of two or more materials consisting of a faceplate and a core layer. The faceplate layer is made of a material with high strength and stiffness, whereas the core layer is made with low strength, stiffness, and density [3]. Currently, the shipbuilding industry uses sandwich panels on approximately 35,000 m^2. The overlay approach has been used extensively in ship repairs, such as on ramps and Ro-Ro decks [4]. Several projects were financed by the European Commission, notably the SAND.CORE has accomplished this objective project [5], which offered the best practices manual for sandwich structures used in marine applications.

A variety of ships can be constructed using sandwich panels. Sandwich materials can be used for ship repair or new construction plans. Each sandwich type has a required standard to fulfill the standardization of material qualities standards and sandwich material strength throughout the development stage of sandwich materials. Classification societies often publish these standards to guarantee high safety and quality requirements. The basis of all marine sandwich construction regulations is guaranteeing that they are similar to their counterparts made of an existing single plate or with steel reinforcement. The guidelines set out by classification agencies include specific strength requirements and an evaluation method to address the variations in reactivity between sandwich and conventional structures [6].

Various studies on the application of sandwich structures in various ship designs due to static and dynamic behavior and weight-saving analysis were studied [7-16]. The expansion of knowledge in both practical and scientific fields shows how the application of sandwich material is distinctly based on the different structural locations and elements. There will be a brief discussion of static and dynamic load structural assessments at various ship structural locations. Tankers with a double bottom, side shell, main deck, and longitudinal bulkhead are being used for cutting-edge research into the usage of sandwich material. Due to the removal of stiffeners from the production process, the results reveal a 2.8% reduction in overall weight and 20% reduction in workload [7]. Moreover, Ismail et al. [8] investigated using a hybrid sandwich made of steel/polyurethane components in a tanker's side shell and deck by adjusting the stiffener frame spacing. Stress reduction and weight loss are possible with a positive result. The structural weight varies between 4.2 and 8.8%, while the promising stress reduction extends from 20.8 to 27.9%. To minimize weight and increase payload, a sandwich panel can eliminate the need for stiffeners [9]. A complete investigation of a structural assessment owing to static and dynamic load in the vehicle deck of a ferry Ro-Ro ship is conducted [10]. Sandwiches with varied stiffener configurations, load types, and material types resulted in stress reductions of nearly 14.6–15.8% and weight savings of roughly 8.87-11.6%. Furthermore, other structural areas on the same ship are being used for the investigation. With stress reductions of up to 28.4% and weight savings of roughly 17.1%, sandwich panels on side shells show promising results [11].

Although the fabrication of sandwich panels appears simple, rigidity and various damage issues need to be considered. The face-core interaction layer is frequently the weakest joint [12]. It is prone to debonding because of the sizable variations in material characteristics and thickness of constitutive materials [13]. It results in significant deformation at the interface layer and internal failure at the outer core material [14], which may compromise the structural integrity [15]. The difficulty in ensuring appropriate bonding during production is one of the factors that led to debonding [16]. Consequently, early-stage damage detection is required.

Finite element modal analysis is one of the alternative methods that can detect the presence of debonding. The numerical result may be proposed as preliminary work to improve detection performance. The basic concept is to compare the modal parameters between intact and damaged models using a variety of dynamic properties, such as natural frequencies [17,18,19], mode shapes [20], frequency response functions (FRF) [21], and time or frequency domain data [22,23,24]. It was mentioned that a review of debonding modeling had been conducted using a different methodology. All of the aforementioned summaries focus solely on debonding in simple structures. It is essential to conduct further study in a complex ship structure such as a barge structure.

Using a sandwich panel system (SPS) is an essential aspect to consider when designing new structures, as it can greatly improve their static and dynamic behavior. SPS is a composite material that consists of two thin external skins, usually made of metal, and a thick inner core made of lightweight material. This unique structure provides high strength and stiffness while reducing the overall weight of the structure. However, it is not enough to simply implement an SPS into the design. It is important to ensure that the proposed model has comparable strength and stiffness to the existing structure to maintain safety and stability. This can be achieved through careful planning, analysis, and testing to ensure that the SPS is properly integrated and meets the required specifications. The study aims to propose an investigation strategy to apply SPS on 155 m barge ship structures by evaluating three proposed framing system variations: transverse, longitudinal, and mixed framing systems based on the Lloyd's Register (LR) standard [25]. The study will compare the stiffness of the existing structure with the proposed framing system using numerical free vibration analysis with ABAQUS software by analyzing eigenvalue and mode shapes. This study provides an understanding of the effectiveness of SPS in barge ship structures and identifies the optimal framing system that will enhance their performance.

Additionally, the study aims to comprehensively investigate the dynamic response of barge structures due to debonding damage by reviewing several parameters, such as damage ratio, location, shape, and depth. It can provide insights into the dynamic behavior of barge structures when subjected to debonding damage and identify critical damage parameters that can help improve the safety and reliability of these structures. The findings of the study can potentially inform the design and construction of barge structures in the future, contributing to the advancement of the shipping industry's safety and performance.

2. MODIFICATION STRATEGY DUE TO SPS APPLICATION / *Strategija modifikacije uslijed primjene SPS-a*

2.1. Ship main particular / *Osnovni detalji broda*

A barge is a ship used to transport dry and liquid bulk. These vessels are commonly used in inland waterways, such as rivers and canals, as well as in coastal areas. Barges come in various sizes and shapes, ranging from small flat-bottomed boats to massive, multi-decked vessels capable of carrying thousands of tonnes of cargo. Barges can be specialized for specific types of cargo, such as petroleum products, grain, or coal. In this case, 155 m barge ship for coal cargo transportation is used as the reference model. The main dimension of the barge with a size of LOA x B x T of 155 m x 45 m x 6.1 m is presented in Table 1. A self-propelling mechanism barge is flat-bottomed to ensure maximum cargo capacity. In addition, the longitudinal framing system and midship section of the barge are depicted in Figure 1.

Table 1 The main dimension of 155 m barge
Tablica 1. Glavne dimenzije teglenice od 155 m

Main particular	Value
Length Overall (LOA)	155 m
Length Perpendicular (LPP)	154 m
Breadth (B)	45 m
Depth (H)	9.5 m
Draft (T)	6.1 m

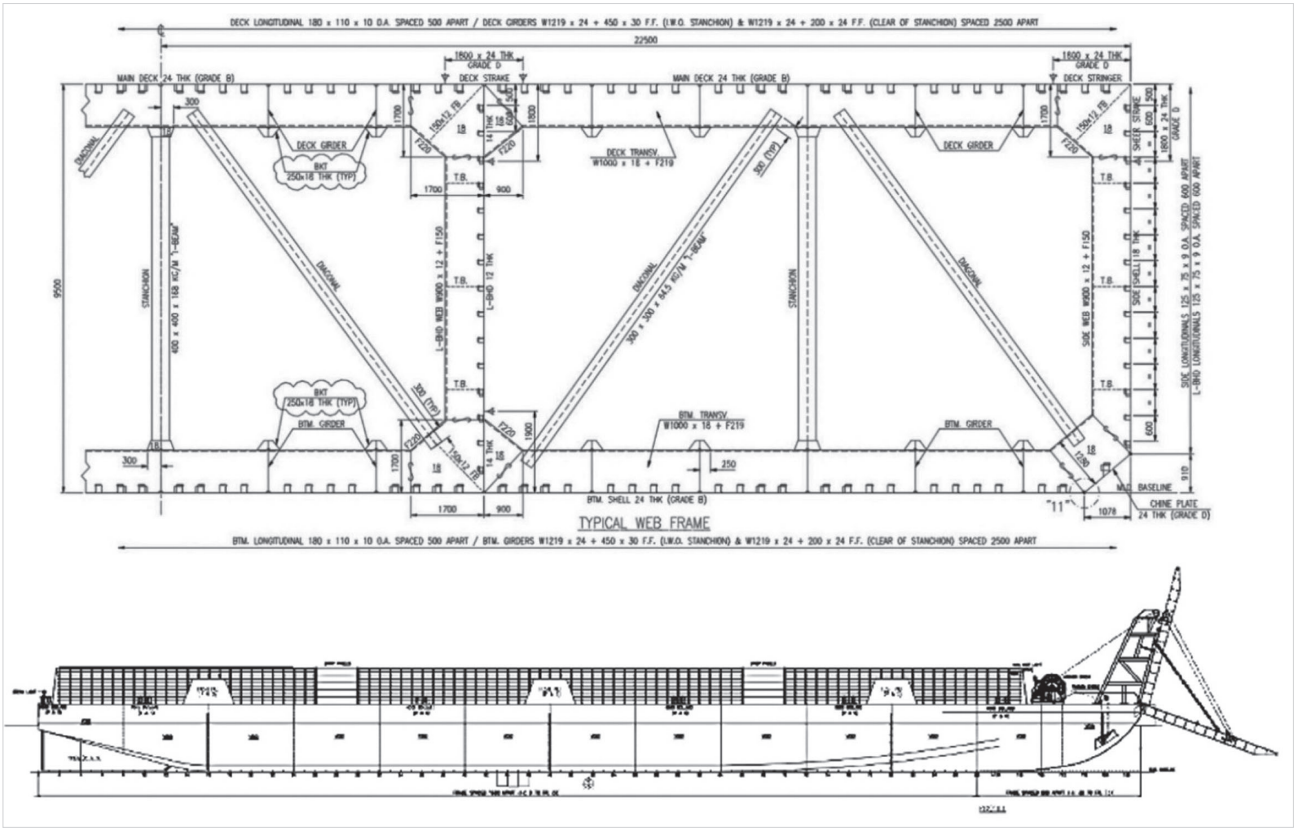

Figure 1 Midship section and framing profile of 155 m barge
Slika 1. Sekcija sredine broda i profil konstrukcije teglenice od 155 m

2.2. Modification of barge framing system / *Modifikacija konstrukcijskog sustava teglenice*

A structural arrangement that reinforces the ship is generally known as a ship framing system. It is ideal for ships to have longitudinal, transverse, and mixed frame systems, depending on the size of the ship. The ship's longitudinal structure supports the framing system, which distributes the load throughout the ship's transverse elements. The principal structural system is installed longitudinally using the longitudinal framing system. This framing technique is suggested for ships longer than 90 meters, according to the Indonesian Classification Bureau's (BKI) standards [26]. A ship framing system that distributes the load transversely is the transverse framing system. Transverse framing systems have transverse main structural components such as web frames, main frames, deck beams, and strong beams and are generally suitable for ships with a length of less than 90 m. In addition, the mixed framing system is a combination of a transverse framing system and longitudinal framing system that is used simultaneously on the deck and bottom of the ship operating a longitudinal framing system while on the side hull using a transverse framing system. Based on BKI, this framing system is recommended for ships with a length of 90 < L < 100 m [26].

The reference framing system of the 155 m barges is a longitudinal framing system. In construction design variations, it is necessary to convert the longitudinal framing system to a transverse and mixed framing system to determine the profile size and cross-sectional modulus. Calculation of the scantling is according to BKI to calculate the size of the profiles such as web frame, main frame, stinger, deck beam, strong beam, and a floor that will be used in the transverse and mixed framing system. The mixed framing system used on the deck and bottom of the ship uses the same profile as the longitudinal framing system, and the sides will use the same frame and web frame as the transverse framing system. Before determining the profile size to be used, it is necessary to calculate the cross-sectional modulus and moment of inertia on each construction under BKI [26].

Based on BKI Vol II Section 5 C.2.1 [26], there are requirements for minimum cross-section and minimum cross-section inertia that must be fulfilled by the ship. The calculated sectional modulus and moment of inertia of the ship will be compared with BKI requirements. If the value obtained exceeds the minimum standards, the ship's longitudinal strength meets the requirements.

2.3. Procedure of SPS application using LR standard / *Postupak primjene SPS-a uporabom LR standarda*

Using the regulations issued by Lloyd's Register [25], modifications to the ship's framing system can be conducted by applying for a sandwich plate with a certain thickness configuration so that the strength has equal value with the existing structure. In the first stage, the value of the existing ship's cross-sectional modulus and moment of inertia is calculated where the value of the cross-sectional modulus of the deck and bottom must be greater than the minimum value.

The calculation procedure of sandwich plate configuration using Lloyd Register is depicted in Figure 2. The calculation step is carried out using the assumption of new building construction, per the provisions contained in the Lloyd Register [7]. The strength index (*R*) must be ≤ 1 to ensure the sandwich configuration has equal strength. The sandwich plate has a minimum core thickness of 15 mm, and the minimum thickness of the upper and lower faceplates can be seen in Table 2.

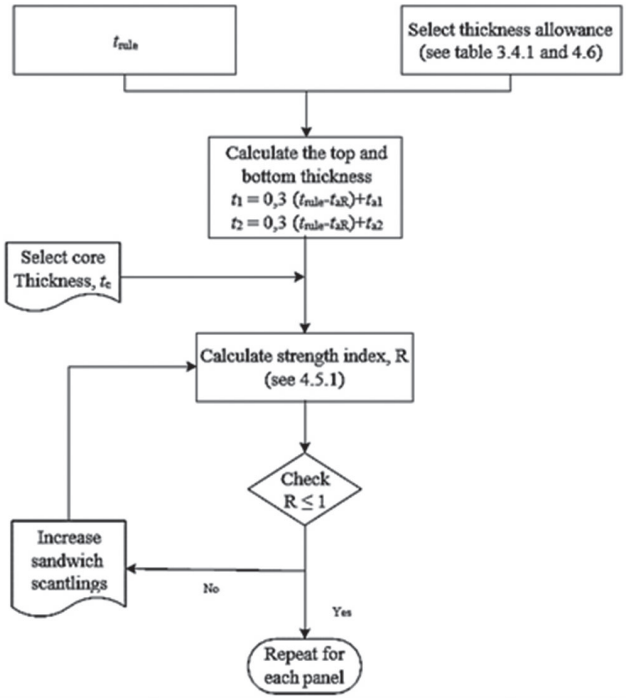

Figure 2 Calculation procedure of scantling size based on LR standard
Slika 2. Postupak izračuna veličine propisanih dimenzija prema LR standardu

Source: [25]

Table 2 Minimum faceplate thickness for new and overlay construction
Tablica 2. Minimalna debljina oplate nove konstrukcije i obloge

Items	Minimum thickness in mm	
	New Construction	Overlay Construction
t_{1min}	3.0	3.0
t_{2min}	3.0	50% of the as-built thickness

Source: [25]

The calculation in Figure 2 is used to compute the thickness of the sandwich plate's faceplate and core. Table 3 displays the strength index value (*R*) data for three different structural sites. The faceplate thickness value for new building configurations is determined by first figuring out the minimum thickness, which is 3 mm. On the bottom and main deck, sandwich plates with a faceplate thickness of 9 mm and core material of 16 mm are used, while the side shell employs sandwich plates with a faceplate and core thickness of 10 mm and 16 mm, respectively.

Table 3 Faceplate and core sandwich thickness of different components
Tablica 3. Debljina oplate i sendvič panela raznih dijelova

Parts	t_c (mm)	*a* (mm)	*b* (mm)	A_R	Z_{rule} (cm³)	*s* (mm)	$P_{eq,R}$ (MPa)	faceplate (mm)			*d* (mm)	*R*
								t_1	t_2	*k*		
Bottom	16	6000	722	3.96	1581207	500	0.10	9	9	1	25	0.6
Side shell	16	6000	600	4.47	158120	600	0.07	10	10	1	26	0.3
Deck plate	16	6000	600	4.47	158120	500	0.11	9	9	1	25	0.5

where *a, b* is the length and breadth of the panel at the longest edge, t_c is the thickness of core material, t_1, t_2 are the thickness of the top and bottom plates, Z_{rule} is equivalent section modulus, *s* is frame spacing, A_R is the ratio of length and breadth of the panel, d is $0{,}5(t_1 + t_2) + t_c$, *Peq,R* is the ratio of section modulus and length of the panel, and *k* is a material factor.

Further calculation in the SPS application is conducted to calculate the sectional modulus and moment of inertia using the sandwich configuration in Table 3. A comparison of sectional modulus and moment of inertia is presented in Tables 4 and 5. It can be found that the proposed SPS model at different framing systems has fulfilled minimum section modulus and moment of inertia criteria.

2.4. Modelling description of barge framing system / *Opis modeliranja konstrukcijskog sustava teglenice*

The ship used as a reference in this research was a 155 m barge ship. Three developed models with different framing systems will be compared with the existing model. The FE model has been simplified by assuming the three cargo holds in the parallel middle body, which has a specified length of 48 m, a width of 22.5 m, and a height of 9 m. In this case, the free vibration analyses are carried out within ABAQUS using the linear perturbation load step and the Lanczos iteration method for eigenvalue extraction [27]. Comparisons of dynamic responses between existing and proposed models are used to assess the effects of SPS addition on modal characteristics. The commercial finite element code ABAQUS/Standard is used to determine the eigenvalues and mode shapes of the models. Three steps constitute the finite element (FE) simulation process: (1) pre-processing, which involves meshing, assembling the mass and stiffness matrices, modeling the geometry of the models, and entering material parameters; (2) a step of linear perturbation analysis, where the frequency is determined using the Lanczos solver. (3) The post-processing step is used to determine the eigenvalues and mode shapes.

The layer-wise solid/shell element can be used to simulate the side hull in the discretization of the finite element model. LR notices that shell elements are used to interpret the faceplate layers, and solid elements are used to interpret the core material [25]. The eight-node quadrilateral shell element (SC8R) was used to simulate the faceplate layers, while the eight-node hexahedral element was used to simulate the core material (3D8I). Shell elements were used to model the stiffeners, which included the mainframe, web frame, side longitudinal, and side stringer (SC8R). Tie constraints modeled contact modeling between all parts of the structure. Meanwhile, the boundary condition should be organized to be the same as the real condition. Fixed support in the rear and front of models, XSYMM (Symmetry in X-axis) in the center of the model, and free in the side model were applied. The boundary condition is depicted in Figure 3.

Material properties of faceplate and core materials used for FEM analysis are presented in Table 6. In this study, the barge construction was replaced by SPS with different thickness configurations and core material types. The core material types consist of fiberglass-reinforced polyurethane (FRPU) and clamshell core material. Both material types were previously developed and published in [28,29]. In FRPU core manufacture, polyurethane elastomer (PU) was formed from a polyurethane prepolymer based on polypropylene glycol (PPG) polyol and MOCA as a curing agent. MOCA is the commercial name for 4,4′-Methylene 2-bis (2-chloroaniline). PPG-based polyurethane elastomer prepolymer and MOCA were imported from Headway Advanced Materials Inc. (Taiwan). A chopped fiberglass mat was purchased from PT. Justus Kimiaraya, Indonesia. Untreated chopped fiberglass of 1 layer fiberglass mat was added using the hand lay-up technique. Density of FRPU core sandwich was obtained by testing the material in the laboratory using Lloyd's Register standard [25]. The ultimate tensile stress, elongation at break, and modulus of elasticity were obtained using the uniaxial tensile test. Moreover, in developing clamshell core sandwich, Yukalac 157 BQTN-EX from PT. Justus Kimiaraya and Methyl Ethyl Ketone Peroxide (MEKP) MEPOXE from PT. Justus Kimiaraya and 30% clamshell powder were used.

Table 4 Comparison of section modulus of different types of framing systems
Tablica 4. Usporedba sekcijskih modula različitih tipova konstrukcijskih sustava

Type of framing system	Sectional modulus (m^3)		Minimum modulus	Criteria	
	bottom	deck	[26] (m^3)	bottom	deck
Conventional - Longitudinal frame system	16.78	16.01	15.15	Pass	Pass
SPS - Longitudinal frame system	20.71	20.49	15.15	Pass	Pass
SPS - Transverse frame system	17.36	16.10	15.15	Pass	Pass
SPS - Mixed frame system	20.59	20.83	15.15	Pass	Pass

Table 5 Comparison of a moment of inertia of different types of framing systems.
Tablica 5. Usporedba inercijskog trenutka različitih tipova konstrukcijskih sustava

Type of framing system	Moment of inertia (m^4)	BKI Minimum moment of inertia [26] (m^4)	Criteria
Conventional - Longitudinal frame system	77.85	70	Pass
SPS - Longitudinal frame system	97.86	70	Pass
SPS - Transverse frame system	79.36	70	Pass
SPS - Mixed frame system	98.37	70	Pass

Table 6 Material properties of the faceplate and core sandwich
Tablica 6. Svojstva materijala oplate i sendvič panela

Materials	Density (kg/m³)	Young Modulus (MPa)	Poisson ratio
FRPU core [28]	1098	901.95	0.36
Clamshell core [29]	1465	44000	0.30
Steel faceplate [30]	7850	210000	0.30

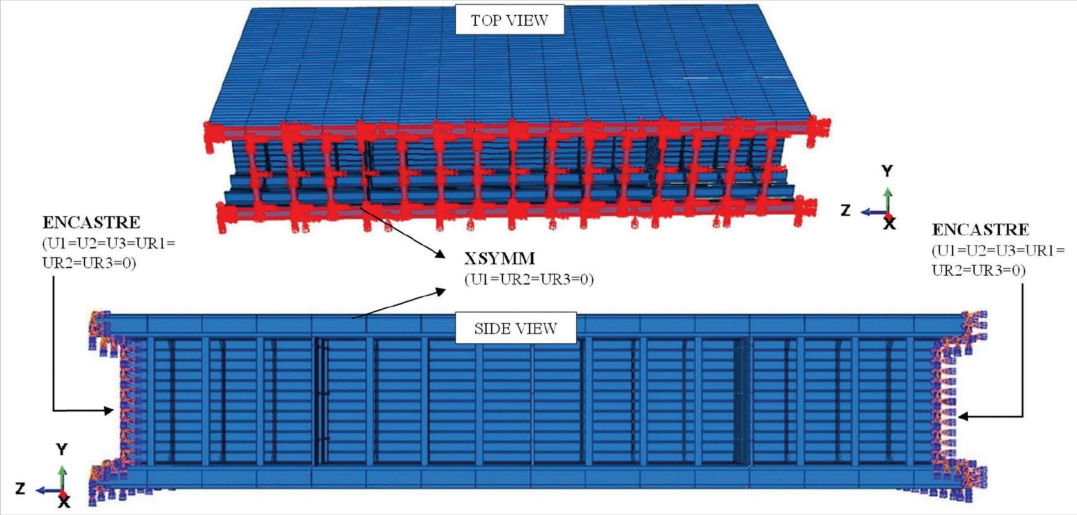

Figure 3 Applied boundary condition on 155 m barge half model
Slika 3. Primijenjeno rubno stanje na polovičnom modelu teglenice od 155 m

Meshing is a simulation process of dividing components into smaller elements. The meshing process affects the results' accuracy and computational time. The smaller the size used in the meshing process, the longer it will take and get more accurate results. On the other hand, using a larger meshing size will take a shorter time and get less accurate results. Figure 5 shows the results of meshing using a structured mesh type. In this study, the convergence analysis was carried out using an eigenvalue variable where the variable must meet the convergence requirements to declare the results valid. To achieve convergence, simulations were carried out on five mesh element sizes starting from 0.6 – 0.1 m. Convergence has been achieved with the number of mesh elements of 741,528 and has a margin of error on the element size 0.1 m of 4.5%.

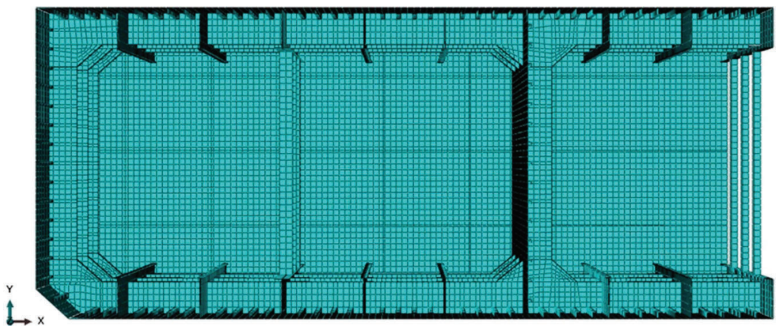

Figure 4 Applied meshing on existing barge structure
Slika 4. Primijenjeno umrežavanje na postojećoj strukturi teglenice

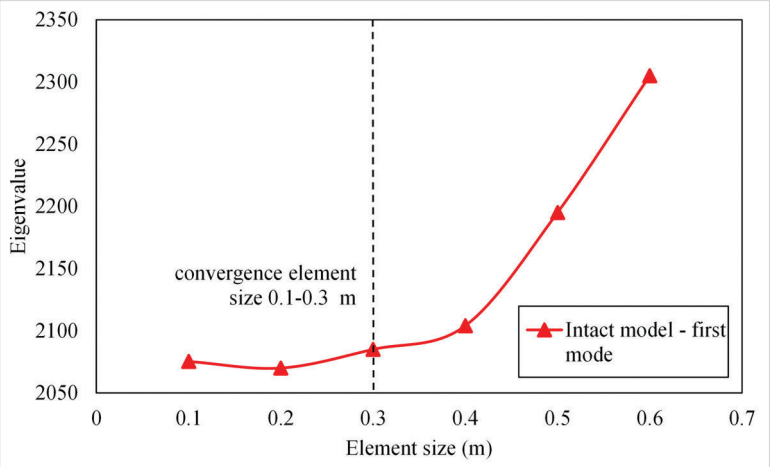

Figure 5 Mesh convergency on the intact model at the first mode
Slika 5. Konvergencija mreža na intaktnom modelu u prvome modu

2.5 Debonding modelling scenario / *Scenarij modeliranja odvajanjem*

Numerous research efforts have been dedicated to examining the vibration responses of sandwich models, utilizing both linear and nonlinear models. However, there appears to be a lack of cohesion in research on modelling the dynamics of sandwich panels with debonding, as it spans various models and research fields. The earliest studies on free vibration utilized the split beam method, where it was assumed that the decoupled layers either freely overlapped or were constrained to move together [31,32]. Later, nonlinear models were developed that improved on this method by accounting for the absence of penetration between the layers that come into contact. Contact models were then developed using the ABAQUS code to handle the behavior between the detached skin and core in both linear and nonlinear dynamic finite element analyses, thereby preventing overlapping. In debonded surfaces, the contact problem has been modeled by linear springs. Additionally, nonlinear analysis can provide insight into the real-life dynamics of debonded sandwich panels by considering the "real contact" conditions between the debonded parts [13].

In the present investigation, debonding is modeled as artificial damage at the interface layer. The debonding ratio is calculated by a damage parameter ($D_{\%}$) designating the ratio of the debonded area, (A_d), to the entire interface layer area of the sandwich, (A_{total}). During the pre-processing, debonding is modeled by creating a gap between two constitutive layers. In the present investigation, spring contact modeling strategies will be applied to prevent overlapping, as depicted in Figure 6a. The spring element (SPRING2) is utilized in ABAQUS [27] to connect two nodes between the faceplate and core layers. According to Figure 6b, the constitutive spring contact used a prior study by Tuswan et al. [33] to predict the behavior of the spring element. When in tension, the stiffness of spring contact is set to zero (k=0 Nm^{-1}) and is assigned to a high value (k=210x10^9 Nm^{-1}) when in compression, that is, when the relative transverse displacement between the face sheet and the core Δu goes to zero. Since any inelastic effects are deactivated for modal analyses [27], we approximate the behaviour of the spring element by its two discrete states as shown in Figure 6b. In such way we are able easily to activate one of the two "contact" options in the modal dynamics. That is, setting a zero stiffness to the spring elements, the contact behaviour of the detached parts is described by the free delamination model; that is, the interfaces move freely, while a nonzero stiffness value of those elements realizes the constrained delamination model between them that restrains the face sheet and the core to move together. So, a contact problem between the face sheet and core in linear dynamic FEAs is reduced to using either "mode constrained" or "mode-free" delamination model [31,32].

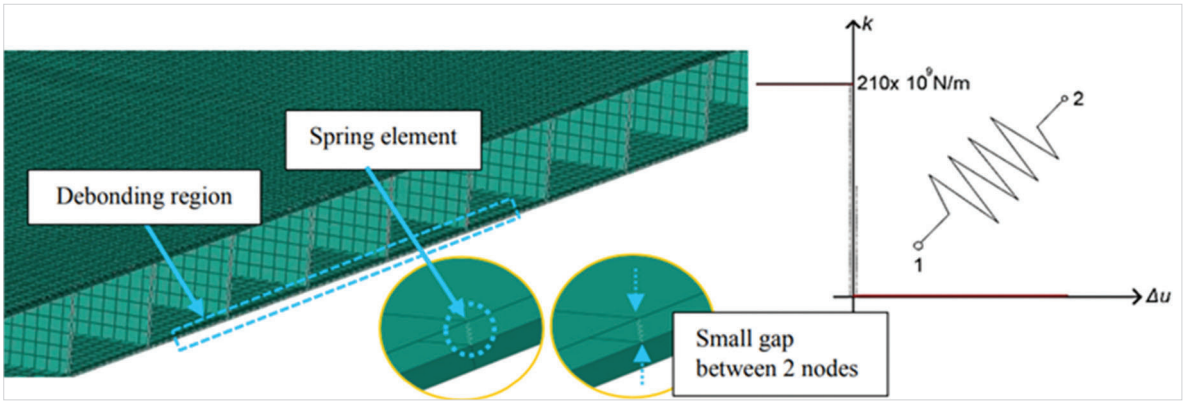

(a) (b)

Figure 6 Spring contact modeling and constitutive spring law
Slika 6. Modeliranje kontaktom opruge i konstitutivni zakon opruge

Table 7 Debonding geometry at different damaged locations
Tablica 7. Geometrija odvajanja na različitima lokacijama oštećenja

Damage ratio ($D_{\%}$)	Debonding geometry (length (l) x width (b) x depth (h)), m		
	Damage located at the bottom structure	Damage located at the side structure	Damage located at the deck structure
10	6.19 x 5 x 0.016	6.19 x 5 x 0.016	6.48 x 5 x 0.016
15	7.74 x 8 x 0.016	7.74 x 8 x 0.016	8.10 x 8 x 0.016
20	10.32 x 9 x 0.016	10.32 x 9 x 0.016	10.80 x 9 x 0.016
25	11.25 x 11 x 0.016	11.25 x 11 x 0.016	11.80 x 11 x 0.016
30	14.07 x 11 x 0.016	14.07 x 11 x 0.016	14.70 x 11 x 0.016

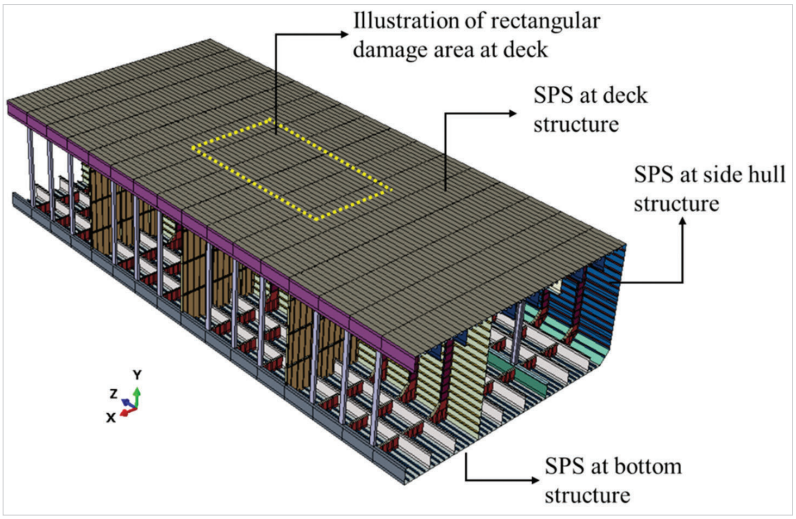

Figure 7 Illustration of damage location at deck structure
Slika 7. Prikaz lokacije oštećenja na strukturi palube

Several assumptions are made when discussing debonding modeling: First, debonding is depicted as artificial damage incorporated into the area where the faceplate and core material meet. Second, the spring contact element is applied between two nodes in the debonded region. Next, it is assumed that debonding is predetermined before vibration starts and that it remains constant throughout vibration. Various regular shapes are used to idealize the shape of the debonded region. In this case, debonding damage in the barge structure is simulated using several damage scenarios. The effect of debonding size, location, shape, and depth on the dynamic response will be investigated. The debonding size is varied with a range of 0-30%, as presented in Table 7. The rectangular debonding shape is used to analyze the effect of debonding ratio.

Moreover, debonding damage is located at three different structural locations, including bottom, side, and deck structures, as seen in Figure 7. In this case, debonding with rectangular shape with 0-30% damage ratio is used to analyze debonding location. Moreover, to investigate the effect of debonding shape to the dynamic responses, damages are varied with different shapes, including rectangular, circular, through-the-width, and through-the-length, as seen in Figure 9. In this scenario, the debonding ratio of 10% is used. Lastly, debonding depth (h) is modeled using 10% rectangular damage with three depth variations: 0.0008 m, 0.001 m, and 0.0014 m. Figure 8 illustrates debonding geometry with debonding depth (h) at the top interface layer.

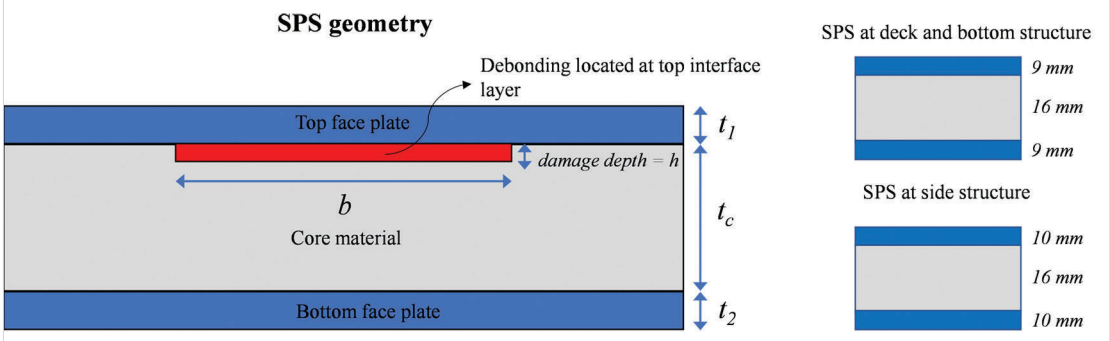

Figure 8 Illustration of debonding geometry at the top interface layer
Slika 8. Prikaz geometrije odvajanja na gornjem međusloju

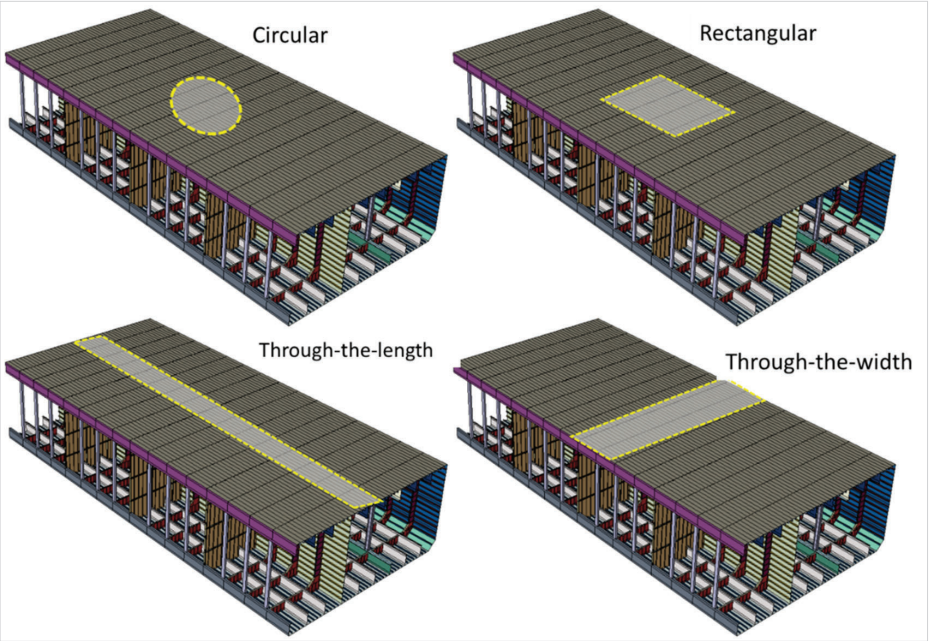

Figure 9 Illustration of debonding shape variations
Slika 9. Prikaz varijacija oblika odvajanja

3. RESULT AND DISCUSSION / *Rezultat i rasprava*

3.1. Comparison of structural weight under different framing systems / *Usporedba strukturalne težine na različitim konstrukcijskim sustavima*

Three types of framing system variations are used such as longitudinal, transverse, and mixed framing systems. The deck, side, and bottom plates of the barge are installed with sandwich plate systems. Figure 10b is a 3D model of SPS with a longitudinal framing system. Variations of the longitudinal framing system use the same framing system as the existing ship in Figure 10a. Longitudinal framing system consists of bottom longitudinal, floor, center, and side girders. Moreover, the deck component consists of deck longitudinal, transverse, center and side deck girder. In the mixed framing system illustrated in Figure 10c, the side structure has the same reinforcing element structure as the transverse framing system. The structure of the reinforcing elements on the sides consists of the main frame, web frame, and side stringer, while the bottom and deck have the same reinforcing element structure as the longitudinal framing system consisting of bottom longitudinal, deck longitudinal, bottom transverse, deck transverse, center and side girder, center and side deck girder, and pillar. Figure 10c is a 3D model of SPS with a mixed framing system. Then, to model the transverse framing system, the reinforcing structural elements on the side structure were initially composed of side longitudinal and side transverse, replaced with frames, web frames, and side stringers. Meanwhile, the deck components initially consisted of deck longitudinal, transverse, side and center deck girders, replaced with deck beams, strong beams, and side and center deck girders. Furthermore, the primary part

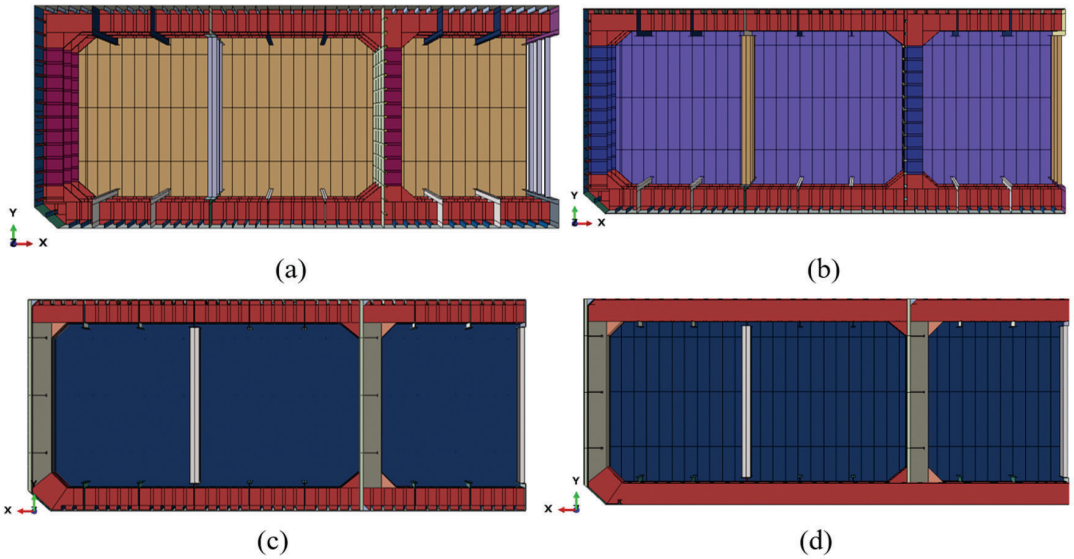

Figure 10 - 3D barge framing system a) Existing-longitudinal framing system, b) SPS-longitudinal framing system, c) SPS-mixed framing system, d) SPS-transverse framing system
Slika 10. 3D konstrukcijski sustav teglenice: a) postojeći uzdužni konstrukcijski sustav, b) SPS uzdužni konstrukcijski sustav, c) SPS miješani konstrukcijski sustav, d) SPS poprečni konstrukcijski sustav

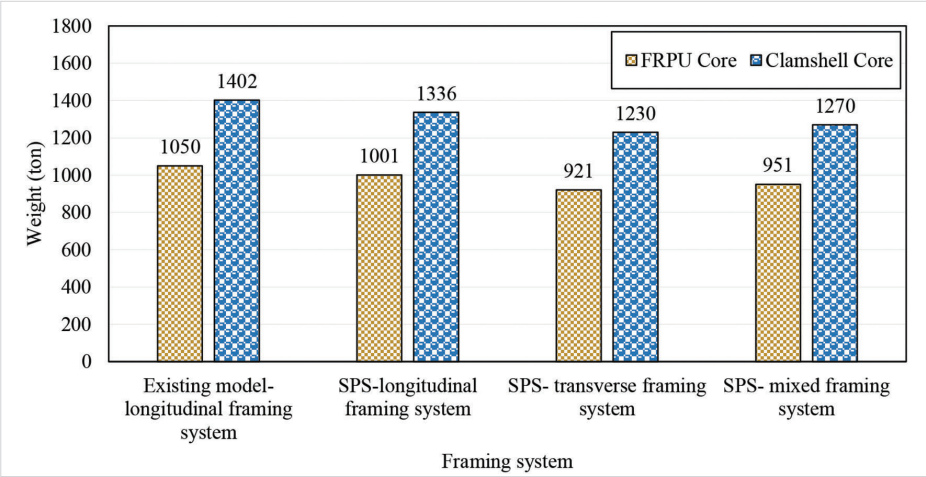

Figure 11 Comparison of structural weight under different framing systems
Slika 11. Usporedba strukturne težine na različitim konstrukcijskim sustavima

of the bottom structure consisted of the bottom longitudinal, bottom transverse, side girder, and center girder are changed to the floor, side girder, and center girder. Figure 6b is a 3D model of the SPS model with a transverse framing system.

To compensate for the increased stress and deformation, the application of sandwich plates in conventional steel plates reduces the structural weight, which can be used to increase the load-carrying capacity. Weight is calculated for all structural elements contained in the model by multiplying the volume value by their respective density. The density of steel is 7.85 $t/m^{3,}$ while the density of FRPU and clamshell core is 1.098 and 1.466 t/m^3, respectively. The weight comparison seen in Figure 11 shows that SPS- FRPU sandwich is lighter than the SPS-clamshell core. The sandwich model with a longitudinal framing system experienced a weight loss of about 5% from the existing ship model. The weight reduction in the longitudinal sandwich model is insignificant because the analysis is carried out globally by only converting the ship's steel plates of the deck, bottom, and sides into sandwich plates without changing the construction structure. Furthermore, it can be seen that the transverse ship framing system and the mixed framing system resulted in a lighter weight of about 13% and 9% than the existing ship model. Both of these can occur due to differences in the use of profile sizes from the longitudinal framing system.

3.2. Comparison of eigenvalue under different framing systems / *Usporedba eigenvalue u različitim konstrukcijskim sustavima*

The finite element results are presented in this section so that the eigenvalue comparison caused by the addition of the sandwich panel may be thoroughly examined. The result of free vibration analysis is conducted to measure the stiffness of different framing systems. The comparison of the first five eigenvalues for different models is presented in Table 8 and Figure 12a for FRPU-Sandwich and Table 9 and Figure 12b for clamshell-sandwich. It can be found from the result that the highest eigenvalue can be found in the existing model. In contrast, the sandwich with a transverse framing system experiences the lowest eigenvalue compared to other framing systems. When subjected to certain external forces, these are

Table 8 Comparison of the first five eigenvalues between the existing model and SPS-FRPU under different framing systems
Tablica 8. Usporedba prvih pet eigenvalues između postojećeg modela i SPS-FRPU u razluičitim konstrukcijskim sustavima

Mode Number	Eigenvalue			
	Existing - longitudinal system	SPS - longitudinal system	SPS- mixed system	SPS - transverse system
1	2075.2	2065.5	2061.2	2056.5
2	2092.9	2083.8	2082.4	2079.4
3	2096.5	2086.6	2090.3	2088.4
4	2467.9	2401.6	2328.6	2290.7
5	2486.5	2419.7	2348.9	2302.9

Table 9 Comparison of the first five eigenvalues between the existing model and SPS-clamshell under different framing systems
Tablica 9. Usporedba prvih pet eigenvalues između postojećeg modela i SPS školjke u različitim konstrukcijskim sustavima

Mode Number	Eigenvalue			
	Existing - longitudinal system	SPS - longitudinal system	SPS - mixed system	SPS - transverse system
1	2075.3	2064.2	2057.2	2051.5
2	2092.9	2080.5	2076.4	2075.4
3	2096.5	2082.3	2084.3	2084.4
4	2467.9	2392.0	2323.6	2284.7
5	2486.5	2421.0	2344.9	2292.9

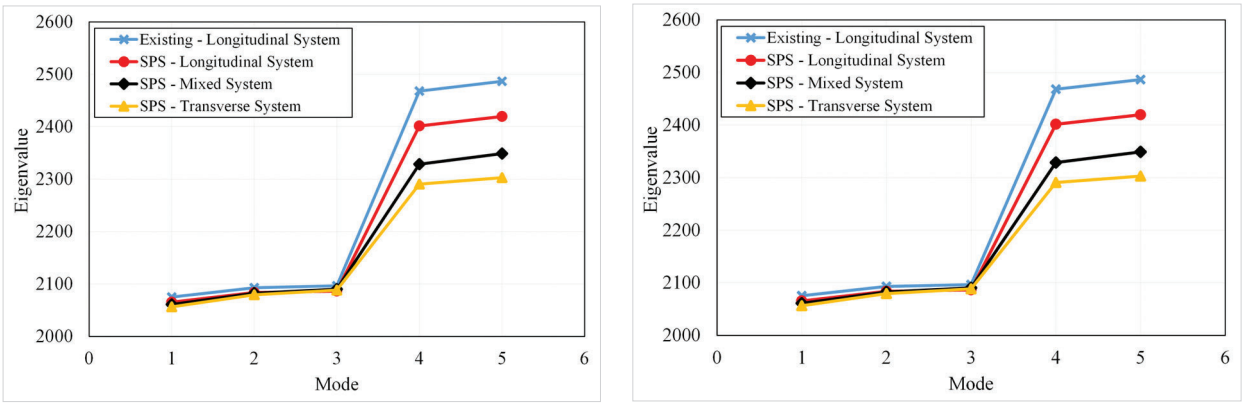

(a) (b)

Figure 12 Comparison of eigenvalues under different framing systems a) FRPU core, b) clamshell core

Slika 12. Usporedba eigenvalues u različitim konstrukcijskim sustavima: a) FRPU okvir, b) školjkasti okvir

the frequencies at which the structure will tend to vibrate. These frequencies are determined by the structure's distribution of mass and stiffness. From Figure 12, it can be evaluated that small frequency discrepancies are found in the first three mode numbers. The frequency of all models tends to have similar values. However, the higher differences in eigenvalues are found in higher modes (modes 4 and 5).

Eigenvalue is the natural frequencies of vibration of a structure, and eigenvalue analysis is used to determine these frequencies and their corresponding mode shapes. In barge design, eigenvalue analysis can help identify potential resonance and vibration issues that may arise due to environmental loads, such as waves or currents, or operational loads, such as cargo or equipment. If the frequency of these loads matches one of the natural frequencies of the barge, it can result in large amplitude vibrations that can damage the structure or cause instability. Eigenvalue is important because it indicates how the natural frequencies of the barge change when additional masses or stiffness are added to the structure. For example, if a barge is designed to carry heavy cargo, the eigenvalue shift analysis can help determine the effect of this additional mass on the natural frequencies of the barge. Similarly, if the barge is equipped with new equipment or machinery, eigenvalue shift analysis can assess the effect of these additions on the dynamic behavior of the barge.

The mode shape of vibration refers to the spatial distribution of vibration amplitudes across a structure vibrating at a particular natural frequency. Each natural frequency has a corresponding mode shape that describes how the object deforms during vibration at that frequency. The mode shape is often represented graphically as a shape or pattern with different colors or contour lines that indicate the magnitude and direction of the vibration amplitudes at different points on the object. Figure 13 compares the mode shapes of the first mode between existing longitudinal framing system model and SPS-clamshell with different framing systems. It can be analyzed that local deformation is located in the same location in the transverse bulkhead. It is caused by the transverse bulkhead plate having the lowest thickness compared to the thickness of the deck, side, and bottom plates. From the result, it can be found that the highest deformation can be found in SPS-clamshell with longitudinal framing system, as seen in Figure 13b.

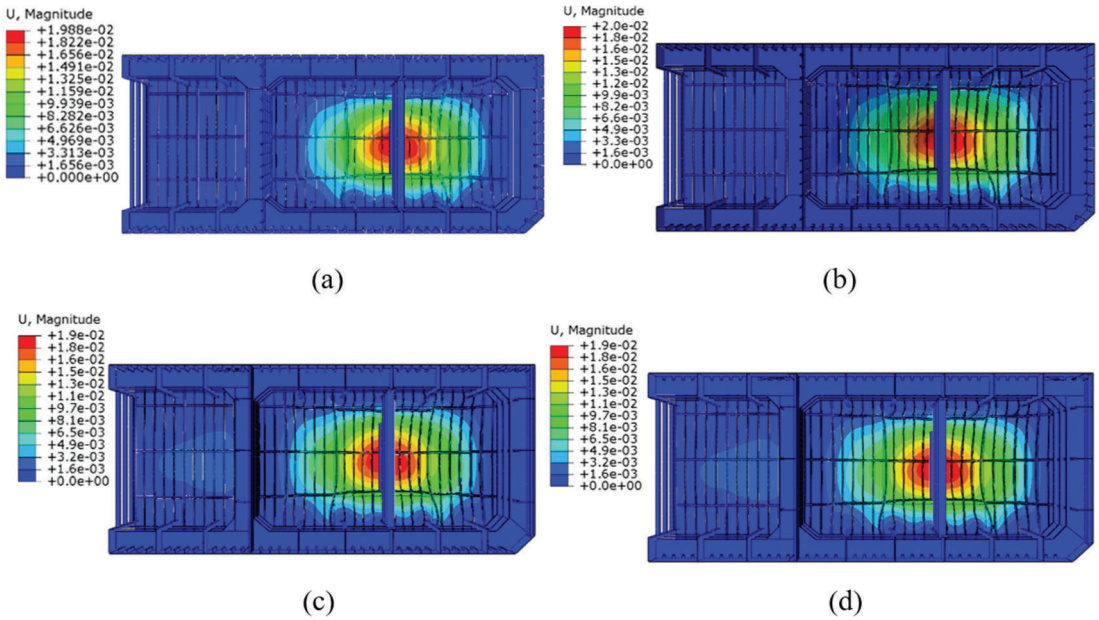

Figure 13 Comparison of displacement on first mode shape a) existing longitudinal framing system, b) SPS-clamshell with longitudinal framing system, c) SPS-clamshell with transverse framing system, d) SPS-clamshell with mixed framing system

Slika 13. Usporedba pomaka na obliku prvog moda: a) postojeći uzdužni konstrukcijski sustav, b) SPS školjkasti uzdužni konstrukcijski sustav, c) SPS školjkasti poprečni konstrukcijski sustav, d) SPS školjkasti miješani konstrukcijski sustav

3.3 Comparison of eigenvalue under different core material types / *Usporedba svojstvenih vrijednosti (eigenvalue) prema različitim vrstama materijala okvira*

This section presents a comparative analysis of the eigenvalue between existing structures and SPS with different core materials. The material properties have a different density, modulus young, and Poisson ratio, as presented in Table 6. Figure 14 compares the eigenvalue of the first ten modes between the existing model and the SPS-longitudinal framing system with FRPU and clamshell core materials. It can be found that the application of the SPS panel to the barge structure results in the same stiffness compared to the existing model. The eigenvalue of the existing model and SPS-FRPU and SPS-clamshell have small discrepancies. The detailed result shows that the SPS application causes a slight eigenvalue increase where the SPS models have a higher eigenvalue than the existing model. The separation of the faceplate by a core material and the different configuration of thicknesses has an impact on the stiffness increase provided on by SPS. This separation results in a large increase in the sectional area and modulus, which can increase bending stiffness.

The comparison of the first mode shape between the conventional structure and the ones equipped with SPS-FRPU and clamshell cores is depicted in Figure 15. The mode shape patterns indicate that in all evaluated models, there is local deformation present in the transverse bulkhead region. The transverse bulkhead plate has the lowest thickness compared to the thickness of the deck, side, and bottom plates, which explains the origin of this deformation. Furthermore, the addition of SPS to the structures results in an increase in stiffness. As observed from the mode shape patterns, the deformation values for SPS-clamshell and SPS-FRPU are lower than the existing model. This suggests that the implementation of SPS technology can improve the structural performance of the vessel, by reducing the deformation and enhancing the stiffness, especially in the transverse bulkhead region. Overall, the mode shape analysis provides valuable insights into the dynamic behavior of structures, and it can aid in the optimization and improvement of the design of various structures, including marine vessels.

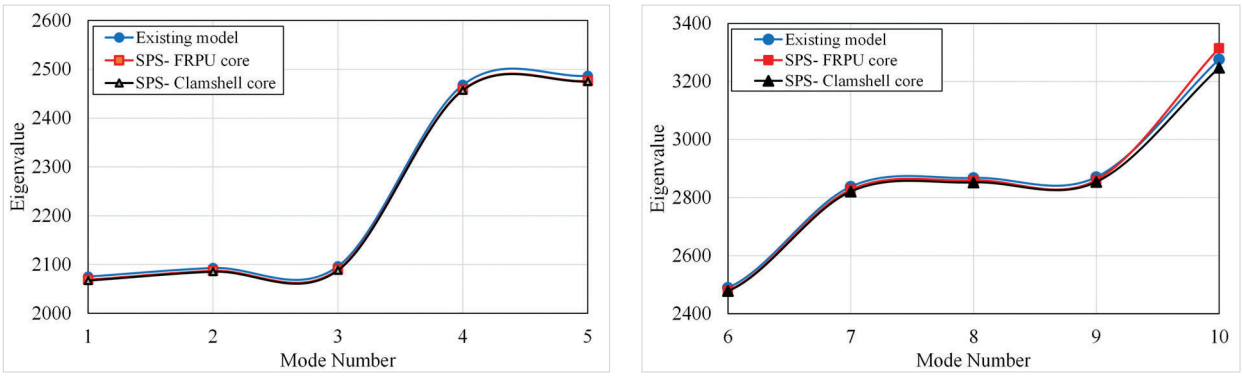

(a) (b)

Figure 14 Comparison of eigenvalue at different core material types a) mode 1-5, b) mode 6-10

Slika 14. Usporedba eigenvalue različitih vrsta materijala okvira: a) mod 1-5, b) mod 6-10

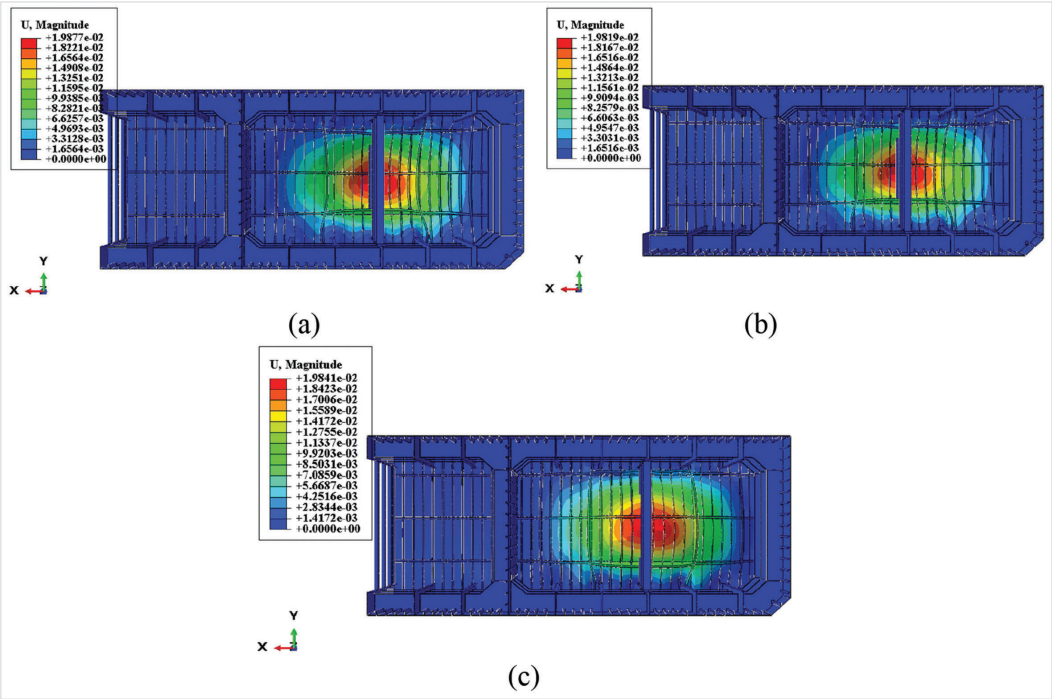

Figure 15 Comparison of first mode shape of a) existing model, b) SPS-clamshell, c) SPS-FRPU

Slika 15. Usporedba oblika prvog moda: a) postojećeg modela, b) SPS školjkastog okvira, c) SPS-FRPU

3.4. Comparison of eigenvalue under different damage ratios / *Usporedba eigenvalue prema različitim stupnjevima oštećenja*

A review of the literature revealed that, despite extensive research on the subject of free vibration of debonding problems, only a small clearer understanding was made regarding predictions of the dynamic properties in terms of the debonding shapes, which were primarily examined in the complex global ship structure.

In this section, the free vibration analysis of rectangular damage shapes at three structural locations will be conducted to investigate the effect of damage ratio on eigenvalue at the deck, side hull, and bottom structures. Figure 16 presents a comparison of eigenvalue as a function of debonding ratio under different ranges of damage ratios at the side hull structure. It can be seen that the eigenvalues primarily decrease as the debonded ratio increases. The eigenvalue reductions increase with increasing damage ratio. In addition, it is clear that compared to the intact model, the presence of debonding ($D_{\%}$=10%) does not substantially alter the eigenvalues. In this case, debonding presence is obviously detected at a higher damage ratio ($D_{\%}$ >10%). Thus, the damage identification to determine the damage in the sandwich plate should be performed in higher mode numbers.

Figure 17 shows that the eigenvalue shifts are more visible in the higher modes compared to the lower modes. The difference between the eigenvalues of the intact model and the damaged model is used to determine eigenvalue shifts. Additionally, it is clear that when the mode number increases, the eigenvalue changes do not follow a monotonous pattern. In summary, the debonding is mode-dependent and can affect natural frequencies. The higher eigenvalue shifts can be found in modes 10, 7, and 8. In contrast, the lower eigenvalue shift is experienced in low mode (modes 1, 2, and 3). The local thickening phenomena carried on by the side hull's debonding violates the trend of frequency change. For the first and second modes with a 10% debonding ratio, the frequency of the damaged model is higher than the initial model. A similar phenomenon can also be seen in the result of modal analysis at the deck and bottom structures in Figures 19 & 21 that the higher the damage ratio, the higher the eigenvalue decrease. It can be found that the eigenvalue of the 10% damage ratio does not almost change compared to the intact model, specifically in low mode (modes 1-3).

Due to the loss of stiffness and strength of the model, the frequency changes of the debonded models increase, and the mode shapes have local deformation in the discontinuity area [33]. A comparison of the first mode shape of rectangular damage at the deck structure is depicted in Figure 22. The deformation contour of the damaged model has local deformation in debonding region. It can be analyzed that the deformation becomes higher as the increase of debonding ratio.

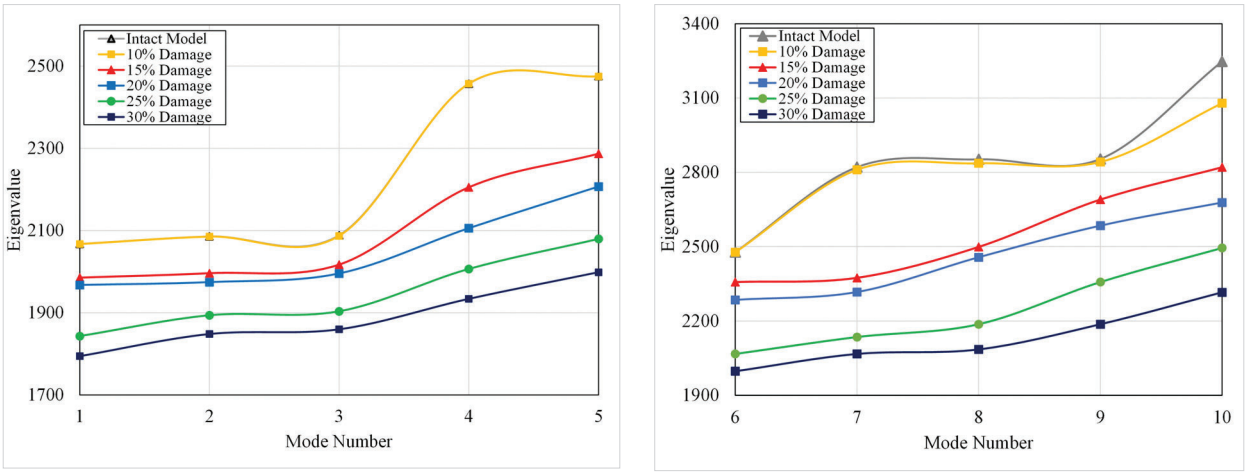

(a) (b)

Figure 16 Comparison of eigenvalue under different damage ratios at side hull a) mode 1-5, b) mode 6-10

Slika 16. Usporedba eigenvalue prema različitim stupnjevima oštećenja na bočnom dijelu trupa: a) mod 1-5, b) mod 6-10

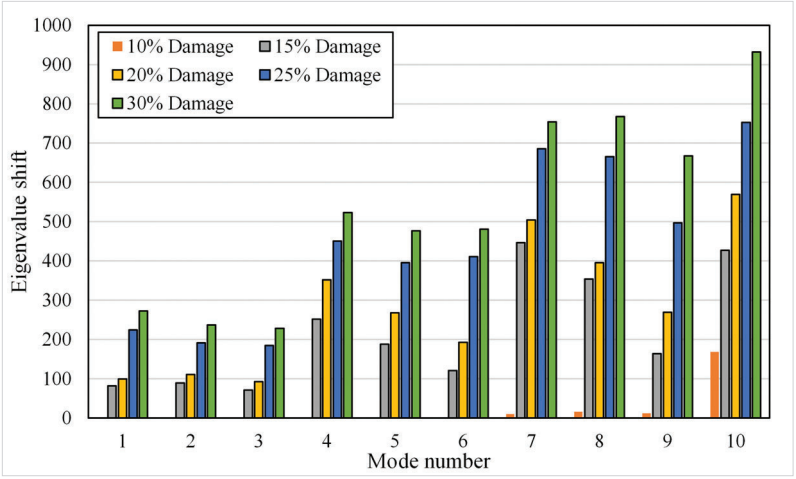

Figure 17 Comparison of eigenvalue shift under different damage ratio at side hull

Slika 17. Usporedba pomaka eigenvalue prema različitim stupnjevima oštećenja na bočnom dijelu trupa

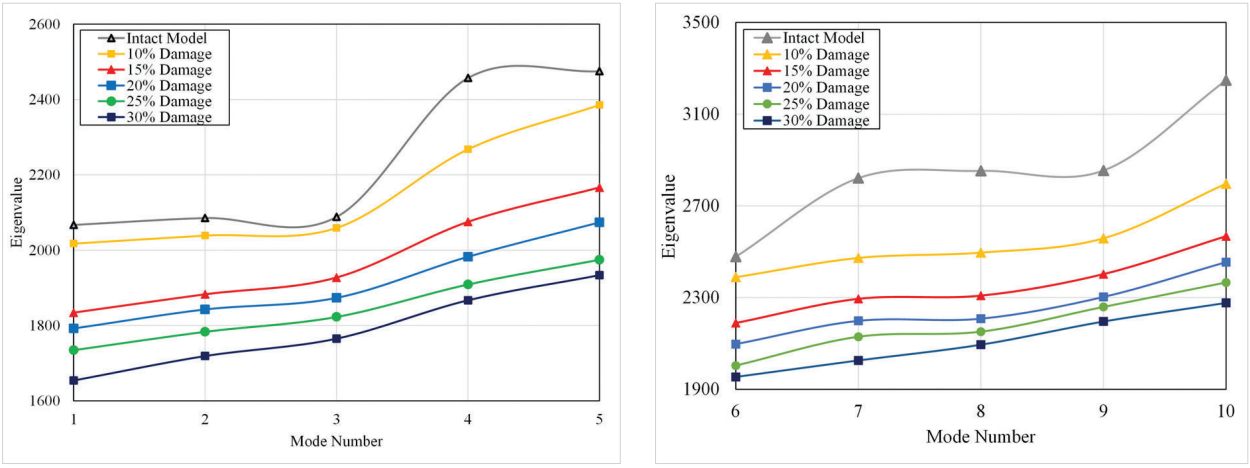

(a) (b)

Figure 18 Comparison of eigenvalue under different damage ratio at bottom structure a) mode 1-5, b) mode 6-10

Slika 18. Usporedba eigenvalue prema različitim stupnjevima oštećenja na strukturi dna: a) mod 1-5, b) mod 6-10

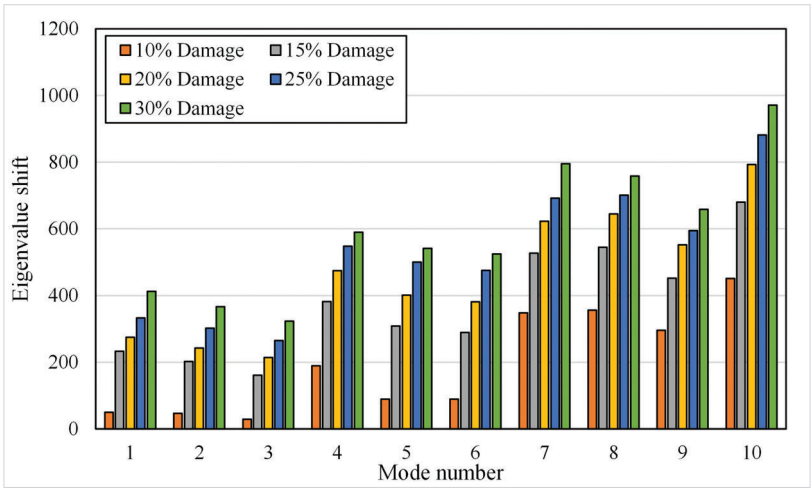

Figure 19 Comparison of eigenvalue shift under different damage ratio at bottom structure

Slika 19. Usporedba eigenvalue pomaka prema različitim stupnjevima oštećenja na strukturi dna

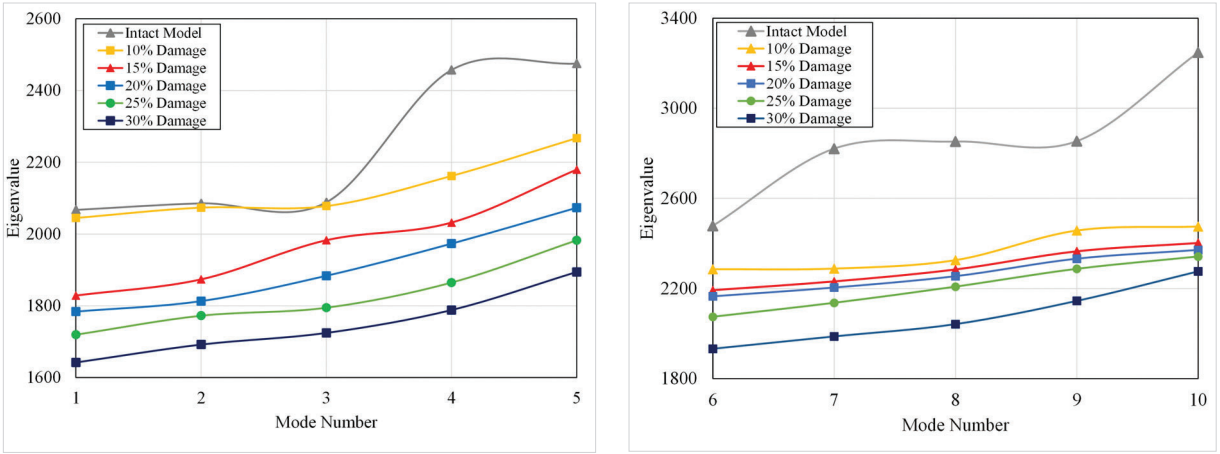

(a) (b)

Figure 20 Comparison of eigenvalue under different damage ratio at deck a) mode 1-5, b) mode 6-10

Slika 20. Usporedba eigenvalue prema različitim stupnjevima oštećenja na palubi: a) mod 1-5, b) mod 6-10

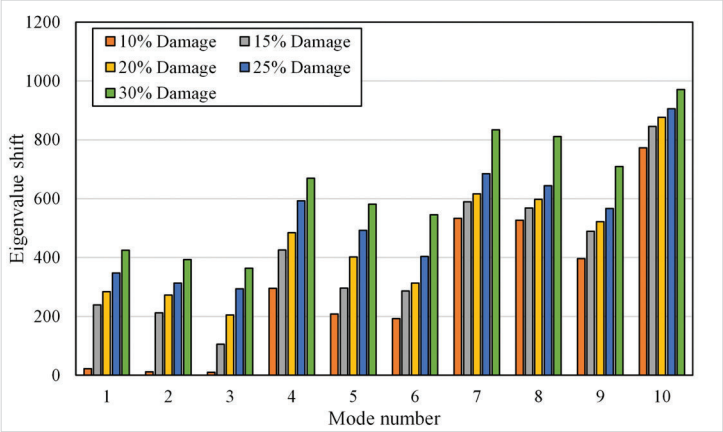

Figure 21 Comparison of eigenvalue shift under different damage ratio at deck structure
Slika 21. Usporedba pomaka eigenvalue prema različitim stupnjevima oštećenja na strukturi palube

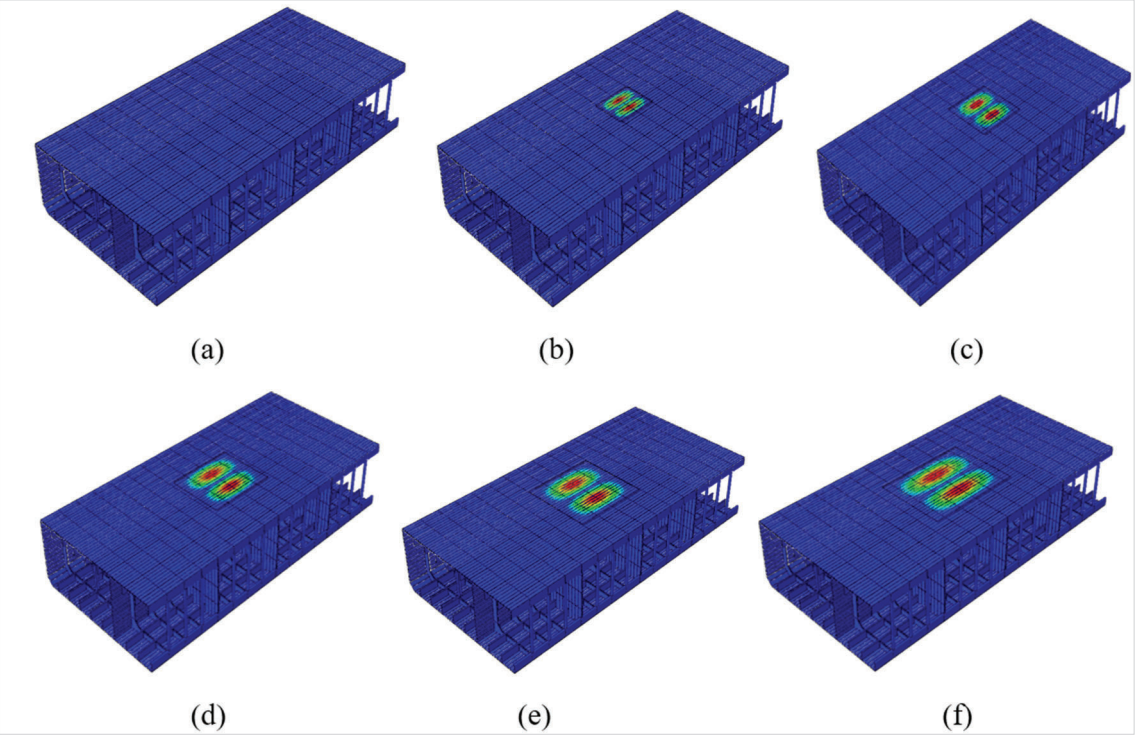

Figure 22 Comparison of first mode shape of rectangular damage at deck a) intact model, b) 10% damage, c) 15% damage, d) 20% damage, e) 25% damage, f) 30% damage
Slika 22. Usporedba oblika prvog moda pravokutnog oštećenja na palubi: a) intaktni model, b) 10% oštećenje, c) 15% ošećenje, d) 20% oštećenje, e) 25% oštećenje, f) 30% oštećenje

3.5 Comparison of eigenvalues under different damage depth / *Usporedba eigenvalues na različitim dubinama oštećenja*

Three rectangular debonding with three variations in debonding depth will be investigated to investigate the effect of debonding depth on the free vibration response. The damage was represented by a 10% damage ratio rectangular debonding found in the deck structure. The model discretization and analytic setup are similar to the prior investigation. The small gap was calculated using debonding depths of 0.014, 0.01, and 0.008 m from the interface layer. Figure 23 compares the finite element predictions for the first ten modes associated with varying debonding depths. It is evident that increasing the debonding depth reduces the eigenvalues marginally. When the debonding depth is increased compared to the initial model, the effect of debonding becomes slightly more obvious. The eigenvalue shifts of the debonded model roughly have similar values between various debonding depths. The eigenvalue shift is happened due to a slight loss in stiffness caused by initial debonding, and the mode shapes cause a local deformation in the debonded area, as seen in Figure 25. The eigenvalue shifts of the debonded model have relatively identical values across different debonding depths. As shown in Figure 25, the eigenvalue shift occurs due to a modest reduction in stiffness induced by early debonding, and the mode shapes produce local deformation in the debonded area.

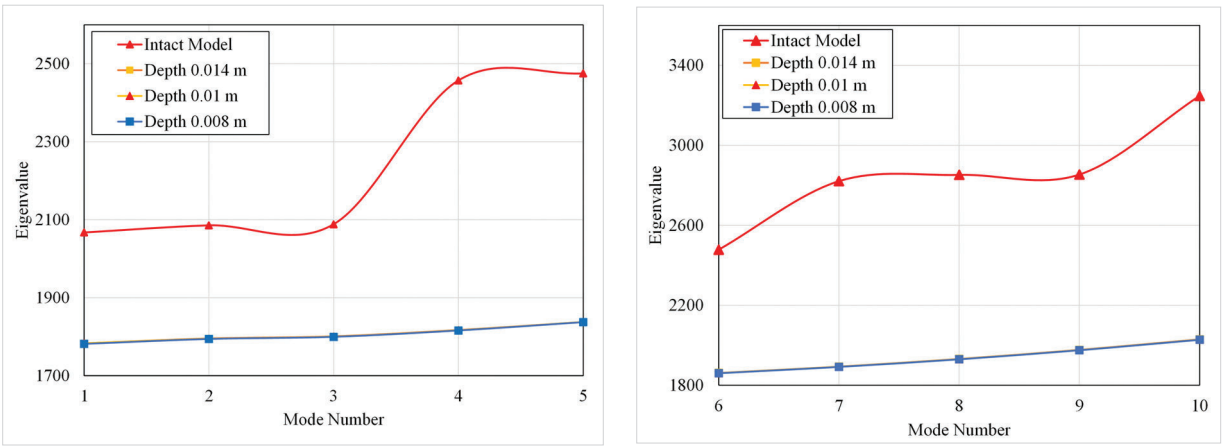

(a) (b)

Figure 23 Comparison of eigenvalue under different damage depths

Slika 23. Usporedba eigenvalue na različitim dubinama oštećenja

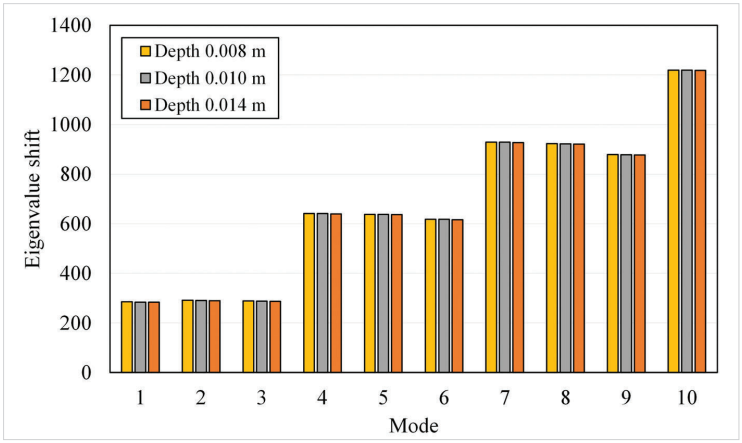

Figure 24 Comparison of eigenvalue shift under different damage depths

Slika 24. Usporedba pomaka eigenvalue na različitim dubinama oštećenja

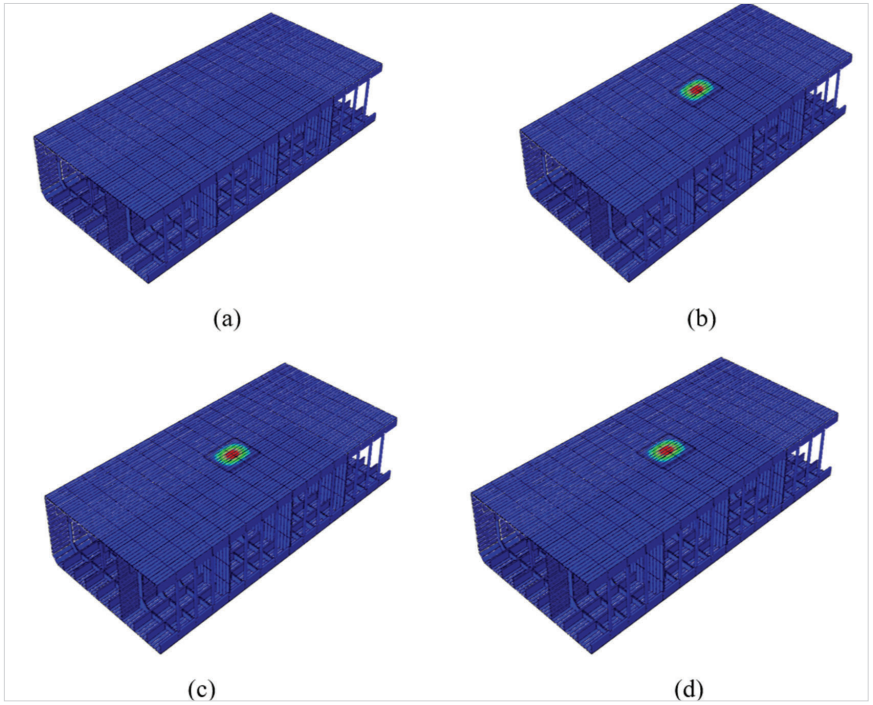

Figure 25 Comparison of first mode shape of rectangular damage at deck a) intact model, b) damage depth 0.014 m, c) damage depth 0.01 m, d) damage depth 0.008 m.

Slika 25. Usporedba oblika prvog moda pravokutnog oštećenja na palubi: a) intaktni model, b) dubina oštećenja 0.014 m, c) dubina oštećenja 0.01 m, d) dubina oštećenja 0.008 m

3.6. Comparison of eigenvalues under different damage shapes / *Usporedba eigenvalues na različitim oblicima oštećenja*

A comparison of the modal characteristics of the barge model to the debonding shape is also investigated. Four types of debonding geometry were explored in the event of interfacial damage: circular, square, through-the-length, and through-the-width. The effect of the equally sized debonding geometry was studied in this section using 30% debonding ratio.

Figure 26 compares the eigenvalues as a function of the debonding geometry. A comparable outcome demonstrates that eigenvalue decreases as a result of debonding damage. Debonding reduces the region where shear stresses are transferred between the faceplate and core, which decreases the stiffness of the model. Interfacial debonding leads to a reduction in eigenvalues, as seen in the results, particularly in the rectangular and circular debonding shapes. In contrast, the through-the-length and through-the-width debonding geometry exhibits no appreciable eigenvalue loss, particularly in the first three modes, as seen in Figure 27. It can be found that the localized debonding types will significantly reduce the eigenvalue compared to the unconfined debonding model. A less amount of damage than in higher modes affects the eigenvalue in the lower mode. The prior study also notes that debonding detection in the sandwich structure is more sensitive in higher modes for small damage [34].

Figure 28 shows the first mode shape between an intact and damaged model with different damage shapes. In the damaged model, there is local deformation in the debonding region. It can be depicted that the shape of local deformation is similar to the debonding shape.

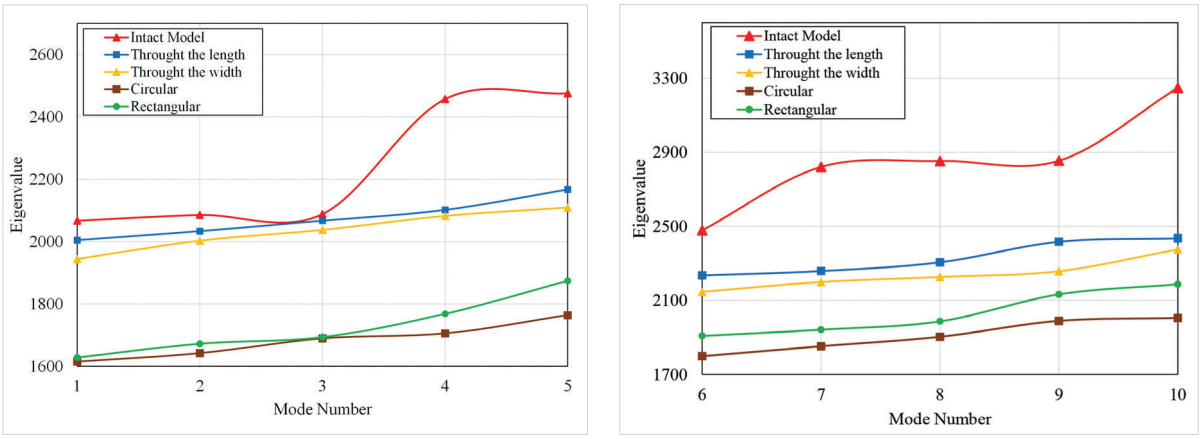

(a) (b)

Figure 26 Comparison of the eigenvalue of different damage shapes a) modes 1-5, b) modes 6-10

Slika 26. Usporedba eigenvalue na različitim oblicima oštećenja: a) mod 1-5, b) mod 6-10

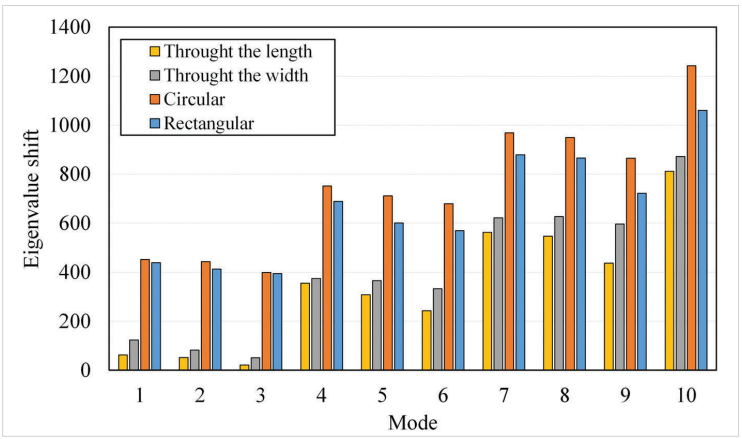

Figure 27 Comparison of first ten eigenvalue shifts of different damage shapes

Slika 27. Usporedba prvih deset pomaka eigenvalue na različitim oblicima oštećenja

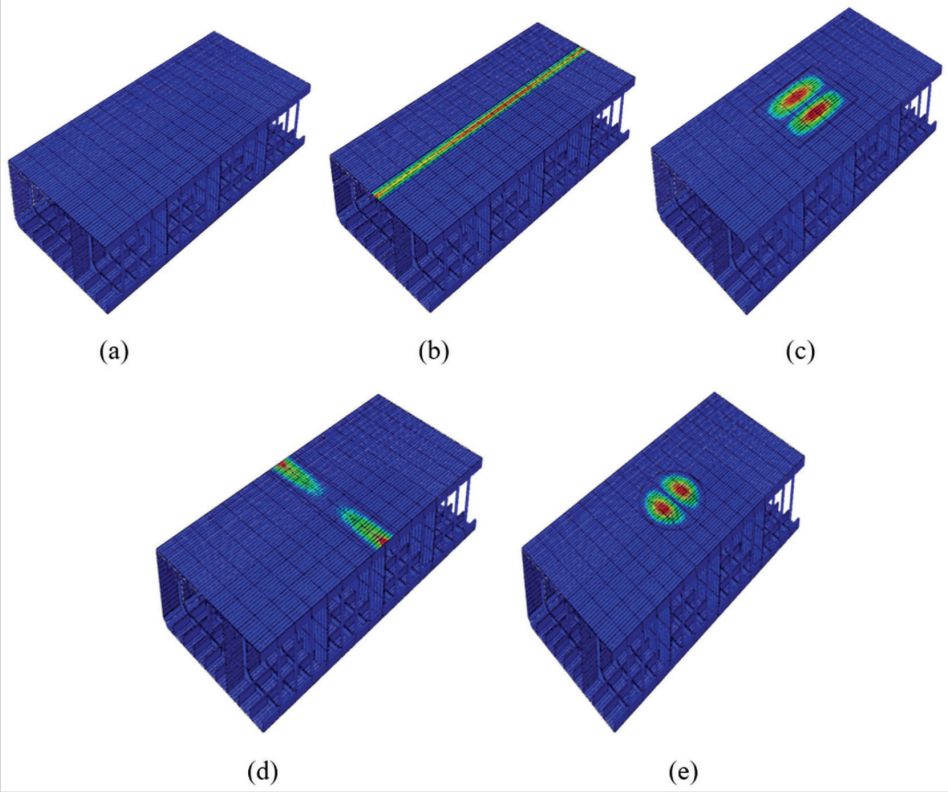

Figure 28 Comparison of first mode shape of different damage shapes a) intact model, b) through-the-length, c) rectangular, d) through-the-width, e) circular

Slika 28. Usporedba prvog moda različitih oblika oštećenja: a) intaktni model, b) po dužini, c) pravokutni, d) po širini, e) cirkularni

4. CONCLUSION / *Zaključak*

The study evaluates the dynamic analysis of different construction systems of barge ships due to applying sandwich panels in different local structures such as the deck, ship hull, and bottom structure of barge ships using Lloyd's Register standard. A total of three proposed construction systems such as longitudinal, transverse, and mixed framing systems, are investigated using free vibration analysis using ABAQUS software. The preliminary study indicates promising sandwich panel application results in a weight saving of about 9-13%. In addition, the application of a sandwich panel on a barge structure slightly has lower stiffness.

In addition, numerous debonding scenarios are examined using free vibration analysis to examine eigenvalue decreases. The results reveal that eigenvalues fall with increasing debonded ratio, and eigenvalue shifts in higher modes are more substantial than in lower modes. Furthermore, interfacial debonding reduces eigenvalues, particularly in rectangular and circular debonding geometries. However, in the through-the-length and through-the-width debonding geometry, there is no significant eigenvalue decrease, particularly in the lower mode. The eigenvalue shifts have roughly identical values at different debonding depths.

Funding: The research has received financial support from the "Riset Publikasi Internasional (RPI), Diponegoro University 2022" research scheme under contract number 569-141/UN7.D2/PP/ VII/2022. The authors gratefully acknowledge the support.

Conflict of interest: None.

Author contributions: All authors have accepted responsibility for the entire content of this manuscript and approved its submission.

Acknowledgments / *Zahvale*

The authors would like to express their gratitude to the Laboratory of Ship Material and Strength at Department of Naval Architecture, Diponegoro University, Indonesia, for providing research facilities and assistance with numerical simulation.

REFERENCES / *Literatura*

[1] Prabowo, A. R., Tuswan T. & Ridwan, R. (2021). Advanced Development of Sensors' Roles in Maritime-Based Industry and Research: From Field Monitoring to High-Risk Phenomenon Measurement. *Applied Sciences*, 11(9), 3954. https://doi.org/10.3390/app11093954

[2] Ismail, A., Zubaydi, A., Piscesa, B., Tuswan, T. & Chandra, A. R. (2021). Study of sandwich panel application on side hull of crude oil tanker. *Journal of Engineering and Applied Science*, 19(4), 1090-1098. https://doi.org/10.5937/jaes0-30373

[3] Borsellino, C., Calabrese, L. & Valenza, A. (2004). Experimental and numerical evaluation of sandwich composite structures. *Composites Science and Technology*, 64, 1709-1715. https://doi.org/10.1016/j.compscitech.2004.01.003

[4] S.CORe. (2013). Best Practice Guide for Sandwich Structures in Marine Applications, 279.

[5] Noury, P., Hayman, B., McGeorge, D. & Weitzenbock, J. (2002). Lightweight construction for advanced shipbuilding-recent development. *Proceedings of the 37th WEGEMT Summer School*, 11-15.

[6] Palomba, G., Epasto, G. & Crupi, V. (2021). Lightweight sandwich structures for marine applications: a review. *Mechanics of Advanced Materials and Structures*, 1-26. https://doi.org/10.1080/15376494.2021.1941448

[7] Brooking, M. & Kennedy, S. (2004). The performance, safety and production benefits of SPS structures for double hull tankers. *Proceedings of the RINA Conference on Double Hull Tankers*. https://doi.org/10.3940/rina.dht.2004.7

[8] Ismail, A., Zubaydi, A., Piscesa, B., Panangian, E., Ariesta, R. C. &Tuswan. (2020). A comparative study of conventional and sandwich plate side-shell using finite element method. *IOP Conference Series: Materials Science and Engineering*, 1034, 012027. https://doi.org/10.1088/1757-899X/1034/1/012027

[9] Momcilovic, N. & Motok, M. (2009). Estimation of Ship Lightweight Reduction by Means of application of Sandwich Plate System. Faculty of Mechanical Engineering, University of Belgrade, Serbia.

[10] Tuswan, Zubaydi, A., Budipriyanto, A. & Sujiatanti, S. H. (2018). Comparative Study on Ferry Ro-Ro's Car Deck Structural Strength by Means of Application of Sandwich Materials. *SciTePress*, 1, 87-96. https://doi.org/10.5220/0008542800870096

[11] Tuswan, Abdullah, K., Zubaydi, A. & Budipriyanto, A. (2019). Finite-element analysis for structural strength assessment of marine sandwich material on ship side-shell structure. *Materials Today: Proceedings*, 13(1), 109-111. https://doi.org/10.1016/j.matpr.2019.03.197

[12] Birman, V. & Kardomateas, G. A. (2018). Review of current trends in research and applications of sandwich structures. *Composites Part B: Engineering*, 142, 221-240. https://doi.org/10.1016/j.compositesb.2018.01.027

[13] Burlayenko, V. N. & Sadowski, T. (2018). Linear and Nonlinear Dynamic Analyses of Sandwich Panels with Face Sheet-to-Core Debonding. *Shock and Vibration,* 1-26. https://doi.org/10.1155/2018/5715863

[14] Mamalis, A. G., Spentzas, K. N., Pantelelis, N. G., Manolakos, D. E. & Ioannidis, M. B. (2008). A new hybrid concept for sandwich structures. Composite Structures, 83(4), 335-340. https://doi.org/10.1016/j.compstruct.2007.05.002

[15] Bragagnolo, G., Crocombe, A. D., Ogin, S. L., Mohagheghian, I., Sordon, A., Meeks, G. & Santoni, C. (2020). Investigation of skin-core debonding in sandwich structures with foam cores. *Materials & Design*, 186, 1-10. https://doi.org/10.1016/j.matdes.2019.108312

[16] Chen, Y., Hou, S., Fu, K., Han, X. & Ye, L. (2017). Low-velocity impact response of composite sandwich structures: modelling and experiment. *Composite Structures*, 168, 322-334. https://doi.org/10.1016/j.compstruct.2017.02.064

[17] Burlayenko, V. N., Sadowski, T. (2010). Influence of skin/core debonding on free vibration behavior of foam and honeycomb cored sandwich plates. *International Journal Non-Linear Mechanics,* 45, 959-968. https://doi.org/10.1016/j.ijnonlinmec.2009.07.002

[18] Zhao, B., Xu, Z., Kan, X., Zhong, J. & Guo, T. (2016). Structural damage detection by using single natural frequency and the corresponding mode shape. *Shock and Vibration,* 1-8. https://doi.org/10.1155/2016/8194549

[19] Ariesta, R. C., Zubaydi, A., Ismail, A. & Tuswan, T. (2022). Identification of Damage Size Effect of Natural Frequency on Sandwich Material using Free Vibration Analysis. *Naše more*, 69(1), 1-8. https://doi.org/10.17818/NM/2022/1.1

[20] Kaveh, A. & Zolghadr, A. (2015). An improved CSS for damage detection of truss structures using changes in natural frequencies and mode shapes. *Advances in Engineering Software*, 80, 93-100. https://doi.org/10.1016/j.advengsoft.2014.09.010

[21] Elshafey, A. A., Marzouk, H. & Haddara, M. R. (2011). Experimental damage identification using modified mode shape difference. *Journal of Marine Science and Application*, 150-155. https://doi.org/10.1007/s11804-011-1054-5

[22] Burlayenko, V. N. & Sadowski, T. (2014). Nonlinear dynamic analysis of harmonically excited debonded sandwich plates using finite element modelling. *Composite Structures,* 108, 354-366. https://doi.org/10.1016/j.compstruct.2013.09.042

[23] Kluczyk, M. & Grządziela, A. (2020). Vibration Diagnostics of Marine Diesel Engines Malfunctions Connected with Injection Pumps Supported by Modelling. *Naše more*, 67(3), 209-216. https://doi.org/10.17818/NM/2020/3.4

[24] Van Hoang, S., & Van Le, V. (2022). Simulating the Torsional Vibration Signal of Two-Stroke Marine Diesel Engine with Normal Firing and Mis-Firing. *Naše more*, 69(3), 143-148. https://doi.org/10.17818/NM/2022/3.4

[25] Llyod's Register. (2015). Provisional Rules for The Application of Sandwich Panel Construction to Ship Structure, UK.

[26] BKI. (2019). Volume II Rules for Hull - Inland Waterways.

[27] ABAQUS. (2016). Abaqus Analysis User Guide, Simulia.

[28] Ismail, A., Zubaydi, A., Piscesa, B. & Tuswan, T. (2023). A novel fiberglass-reinforced polyurethane elastomer as the core sandwich material of the ship plate system. *Journal of Mechancial Behavior of Materials* (in press).

[29] Tuswan, T., Zubaydi, A., Piscesa, B., Ismail, A., Ariesta, R. C. & Prabowo, A. R. (2022). A numerical evaluation on nonlinear dynamic response of sandwich plates with partially rectangular skin/core debonding. *Curved and Layered Structures*, 9(1), 25-39. https://doi.org/10.1515/cls-2022-0003

[30] Lee, C. S., Cho, J. R., Kim, W. S., Noh, B. J., Kim, M. H. & Lee, J. M. (2013). Evaluation of sloshing resistance performance for LNG carrier insulation system based on fluid-structure interaction analysis. *International Journal of Naval Architecture and Ocean Engineering*, 5, 1-20. https://doi.org/10.2478/IJNAOE-2013-0114

[31] Tracy, J. J. & Pardoen, G. C. (1989). Effect of delamination on the natural frequencies of composite laminates. *Journal of Composite Materials*, 23(12), 1200-1216. https://doi.org/10.1177/002199838902301201

[32] Jian, S. H. & Hwu, C. (1995). Free vibration of delaminated composite sandwich beams. *AIAA Journal*, 33(10), 1911-1918, https://doi.org/10.2514/3.12745

[33] Tuswan, T., Zubaydi, A., Piscesa, B., Ismail, A. & Ilham, M. F. (2020). Free vibration analysis of interfacial debonded sandwich of ferry ro-ro's stern ramp door. *Procedia Structural Integrity*, 27, 22-29. https://doi.org/10.1016/j.prostr.2020.07.004

[34] Burlayenko, V. N. & Sadowski, T. (2011). Dynamic behaviour of sandwich plates containing single/multiple debonding. *Computational Materials Science*, 50, 1263-1268. https://doi.org/10.1016/j.commatsci.2010.08.005